ORIGINAL PAPER

Direct measurement of unsaturated permeability of kaolin-sand mixtures

Arezoo Rahimi[1] · Harianto Rahardjo[2]

Abstract

Unsaturated permeabilities of six different kaolin-sand mixtures named as 100K0S, 90K10S, 80K20S, 50K50S, 20K80S, and 10K90S were directly measured using a modified flexible wall triaxial permeameter system. 90K10S means that the soil mixture contains 90% kaolin and 10% sand by dry mass. Soil–water characteristic curves (SWCC) of the kaolin-sand soil mixtures were also measured for a wide range of suctions using a Tempe pressure cell, 5-bar pressure plate, 15-bar pressure plate, and saturated salt solutions. The unsaturated permeabilities of the soil mixtures were also estimated using ten different theoretical models using (1) the measured SWCC data over a complete suction range and (2) the measured SWCC data up to 100 kPa suction in combination with the estimated SWCC data at higher suction values. The directly measured unsaturated permeability of the soil mixtures was used to validate the estimated values of unsaturated permeability. The results showed that the unsaturated permeability estimation models could reasonably fit the directly measured unsaturated permeability data when both the data from the complete measurement of SWCC and the measured SWCC data up to 100 kPa suction in combination with the estimated SWCC data at higher suction values were used.

List of notations

g	Gravitational acceleration
k_r	Relative permeability
k_s	Saturated permeability
k_w	Unsaturated permeability with respect to water
k	Total unsaturated permeability
k_b	Permeability of bottom disk
k_t	Permeability of top disk
L	Total length of the three layers
L_b	Length of the bottom disk
L_s	Length of the soil specimen
L_t	Length of the top disk
L_a	Apparent or macroscopic path length
$RMSE$	Root mean square error
T_s	Surface tension
ρ_w	Density of water
u_a	Pore-air pressure
u_w	Pore-water pressure
$u_a - u_w$	Matric suction
wc	Gravimetric water content
y_i	A measured or observed value
$\hat{y}_i$	A predicted value by a model
y_{imin}	Minimum measured or observed value
y_{imax}	Maximum measured or observed value
ψ	Soil suction

✉ Arezoo Rahimi
Arezoo.rahimi@auckland.ac.nz
https://profiles.auckland.ac.nz/arezoo-rahimi

1 Department of Civil and Environmental Engineering, University of Auckland, Auckland 1010, New Zealand

2 School of Civil & Environmental Engineering, Nanyang Technological University, Singapore, Singapore

Introduction

Unsaturated permeability of soil is either directly measured in soil laboratories or estimated by the available theoretical models from soil–water characteristic curve (SWCC) (van Genuchten 1980; Fredlund et al. 1994; Samingan et al. 2005; Cihan et al. 2009; Liang et al. 2018; Bhaskar et al. 2022). The SWCC and saturated permeability of the soil are measured in the laboratory, and then, the unsaturated permeability function is estimated from those measurements (Brutsaert 1966; Fredlund et al. 1994; Mualem 1976; van Genuchten 1980). On the other hand, the direct measurements of unsaturated permeability of soils should be performed by

a well-trained technician and it requires expensive equipment and tremendous amount of time (van Genuchten 1980; Samingan et al. 2003; Chaminda et al. 2013; Pandey et al. 2021). Therefore, the estimation models are usually preferred. However, a reliable estimation of the unsaturated permeability of soil by theoretical models depends on the input factors of the estimation models (Rahimi 2015). Unsaturated permeability estimation models are obtained by combining any pair of best-fit soil–water characteristic curve (SWCC) equation and relative permeability equation (k_r). The saturated permeability of soil is then multiplied by the estimated unsaturated relative permeability function. As a result, relative permeability equation, best-fit SWCC equation, and measured SWCC data are considered as the input factors of any unsaturated permeability estimation models (Rahimi 2015). Table 1 shows a matrix of unsaturated permeability estimation models containing twelve different estimation models developed by Rahimi et al. (2015a).

In this study, unsaturated permeabilities of six different kaolin-sand mixtures were directly measured using a modified flexible wall triaxial permeameter system. The SWCCs of the kaolin-sand soil mixtures were also measured over a wide suction range using a Tempe pressure cell, 5-bar pressure plate, 15-bar pressure plate, and saturated salt solutions. The matrix of estimation models as shown in Table 1 was used to predict the unsaturated permeabilities of the six kaolin-sand soil mixtures using the measured input factors.

Rahimi et al. (2015b) showed that the choice of best-fit SWCC equations and relative permeability equations greatly affected the estimated unsaturated permeability functions. However, the most significant effective input factor was the range of measured SWCC. It was shown that a complete measured SWCC could result in a more reliable estimation of the unsaturated permeability functions. Since the complete measurement of SWCC may not be practical due to the lengthy testing time and different equipment requirements, a method which uses the grain size distribution curve and the measured SWCC data at 100 kPa suction was proposed to estimate the SWCC data points beyond 100 kPa suction to complement the limited measurements of SWCC (Rahimi and Rahardjo 2015).

The unsaturated permeabilities of the kaolin-sand soil mixtures were estimated using three different SWCCs. First, the data of the complete measurement of SWCC were used as the input for the estimation. Second, only the data of the measurement up to 100 kPa suction were used as the input for the estimation. Third, the data of the measurement up to 100 kPa in combination with the estimated SWCC data points (i.e., beyond 100 kPa suction) were used as the input for the estimation. The estimated unsaturated permeability functions of soil mixtures obtained from three different approaches were validated against the directly measured unsaturated permeability of the soil mixtures.

Experimental study

An experimental program consisting of basic soil properties characterization tests and two main tests, SWCC tests, saturated, and unsaturated permeability tests were conducted on six different soil mixtures of coarse kaolin and fine sand. Coarse kaolin produced by Kaolin Malaysia SDN BHD (Malaysia), and Ottawa sand furnished by the U.S. Silica Company, were selected and mixed for producing the soil specimens. In order to ensure that experimental results are reliable and reproducible, soil specimens for each soil mixture were required to be identical for all the tests (i.e., SWCC tests and unsaturated permeability test). Therefore, uniform and homogeneous soil specimens were prepared at similar initial water content and initial dry density in the different tests, in order to produce meaningful results for comparisons and analyses. Six different kaolin-sand mixtures named as 100K0S, 90K10S, 80K20S, 50K50S, 20K80S, and 10K90S

Table 1 Matrix of unsaturated permeability estimation models

SWCC		k_r		
		Childs and Collis-George	Burdine	Mualem
		C	**B**	**M**
Fredlund and Xing (1994)	**F**	Fredlund et al. (1994), FCM[*]	FBM	FMM
Fredlund and Xing (1994) with $C(\psi) = 1$	**F, $C(\psi) = 1$**	FCM ($C(\psi) = 1$)	FBM ($C(\psi) = 1$)	FMM ($C(\psi) = 1$)
van Genuchten (1980)	**V**	VCM	VBM	VMM
van Genuchten (1980) with m = 1–1/n	**V, $m = 1 - 1/n$**	VCM ($m = 1 - 1/n$)	VBM ($m = 1 - 1/n$)	(van Genuchten 1980), VMM ($m = 1 - 1/n$)

[*]FCM means that the model resulted from the combination of Fredlund and Xing's best-fit SWCC equation and Childs and Collis-George relative permeability equation. The capital M at the end of each name stands for model. Therefore, FCM refers to the Fredlund and Xing-Childs and Collis-George model. The rest of the names can be interpreted according to this description

were used. 90K10S means that the soil mixture contains 90% kaolin and 10% sand by dry mass.

Basic soil properties

Basic soil properties tests according to ASTM (1997) soil testing standard were performed on all soil mixtures. Table 2 summarizes all the basic soil property test results.

Soil mixtures 100K0S, 90K10S, 80K20S, 50K50S, 20K80S, and 10K90S were classified as MH, CL, CL, SC, SM, and SP-SM respectively, according to the Unified Soil Classification System (ASTM D2487-93). The first three soil mixtures were closely located to "A" line in Casagrande plasticity chart. Static compaction was used to prepare the soil specimens with a height of 30 mm and a diameter of 50 mm for SWCC and permeability tests. The soil specimens were prepared at the maximum dry density (ρ_{dmax}) and optimum water content (w_{opt}) where a tolerance interval of $\pm 5\%$ of the maximum dry density was allowed.

Soil–water characteristic curve tests

The soil–water characteristic curve (SWCC) of all the soil specimens were measured over a large suction range using a Tempe pressure cell, 5-bar pressure plate, 15-bar pressure plate, and saturated salt solutions. The SWCC tests were performed under zero net confining pressure. The specimen was first prepared and placed in the Tempe cell to reach saturation. The saturation was performed by connecting the bottom of the Tempe cell to a flexible tube that was connected to a burette filled with distilled and de-aired water. The level of water in the burette was slightly above the level of the ceramic disk. The water flowed to the bottom of the soil specimen through the pre-saturated ceramic disk. It should be noted that the ceramic disk was saturated by submerging it into the distilled and de-aired water in a vacuum desiccator for a few days. The needed water for saturation was computed by considering the volume-mass relationships. The mass of the Tempe cell was measured regularly to assure that the soil specimen was saturated. It should be noted that the water level in the burette was checked regularly to ensure there was no water loss due to evaporation. The axis-translation technique (Hilf Jack 1956) was then used to apply suction to the saturated soil specimen. At the last target value of 90 kPa (after the equilibrium condition was achieved), the soil specimen was transferred from the Tempe cell to the 5-bar pressure plate. An air pressure of 100 kPa was applied and zero water pressure condition (i.e., the water level in the connected burette was kept the same as the level of the ceramic disk). The soil specimen mass was measured daily and plotted versus time. The air pressure was increased to the next target pressure once the equilibrium condition was reached. Once the equilibrium condition was achieved at the last target air pressure of 450 kPa, the soil specimen was transferred to the 15-bar pressure plate. An air pressure of 500 kPa was applied after the soil specimen was transferred to the 15-bar pressure plate, and similar procedure was followed for each target air pressure. At the last target pressure of 1400 kPa (after the equilibrium condition was achieved), the soil specimen was dried in an oven for 24 h to correct the initially computed dry mass according to the mass-volume relationship.

The soil specimens with a height of 10 mm and a diameter of 50 mm were prepared and saturated. The salt solution method was then used to measure SWCC at high-suction values. The

Table 2 Soil properties of kaolin-sand mixtures

Soil properties of soil mixtures	100K0S	90K10S	80K20S	50K50S	20K80S	10K90S
Maximum dry density, ρ_{dmax} (Mg/m^3)	1.40	1.54	1.6	1.75	1.94	1.84
Optimum water content, w_{opt} (%)	23.9	21.8	18.9	12.5	9.2	8.3
Specific gravity, G_s	2.67	2.67	2.67	2.67	2.66	2.66
Liquid limit (LL)	50.20	45.88	41.19	27.68	15.86	15.69
Plastic limit (PL)	30.29	26.76	23.9	19.44	N.A	N.A
Plasticity index (PI)	19.91	19.12	17.29	8.24	N.A	N.A
Sand (4.75 ~ 0.075) mm (%)	0	9.99	19.97	49.93	79.89	89.87
Silt (0.075 ~ 0.002) mm (%)	90.63	82.00	72.91	45.62	18.33	9.24
Clay (< 0.002) mm (%)	9.37	8.01	7.12	4.45	1.78	0.89
D_{60} (mm)	0.0187	0.02	0.024	0.32	0.41	0.42
D_{30} (mm)	0.009	0.0115	0.014	0.02	0.28	0.32
D_{10} (mm)	0.0025	0.005	0.003	0.005	0.015	0.072
$C_{U\ (D60/D10)}$	7.48	4	8	64	27.3	5.83
C_c ($D_{30}^2/D_{60}D_{10}$)	1.73	1.32	2.72	0.25	12.75	3.39
USCS symbol	MH	CL	CL	SC	SM	SP-SM
Saturated permeability, k_s (m/s)	1.87 10^{-8}	8.02 10^{-8}	1.67 10^{-7}	2.7 10^{-7}	8.80 10^{-7}	1.27 10^{-5}

soil specimen was put into a ceramic crucible and together placed in a desiccator in order to be in equilibrium with the water vapor associated with the salt solution concentration. The soil specimen with the ceramic crucible was weighed weekly until there was no change in the mass of the soil specimen and equilibrium condition was achieved. The soil specimens were then dried in an oven for 24 h to correct their initial dry masses according to the mass-volume relationship.

Direct unsaturated permeability tests

Unsaturated and saturated permeability tests were conducted for all the six soil mixtures prepared in this study. The saturated permeability tests were conducted using the constant-head method according to D5084 (ASTM 2003). The unsaturated permeability tests were conducted using a triaxial apparatus designed for unsaturated soil testing as described by Fredlund and Rahardjo (1993). The triaxial system was modified based on modifications performed by Goh et al. (2015). Figure 1 shows a schematic diagram of the triaxial permeameter.

As shown in the figure, the triaxial permeameter used in this study consists of a transparent triaxial cell, top cap, ceramic disks, pedestal, pore-air pressure control system, a digital pressure and volume controller (DPVC) for cell pressure (i.e., confining pressure), two digital pressure and volume controllers (DPVC) for pore-water pressure, a diffused air volume indicator (DAVI), four pressure transducers, thermal sensor, data acquisition system, and a computer. The

pedestal was made of stainless steel and the top cap was made of aluminum. Spiral grooves were constructed inside the top cap and water compartments of the pedestal. Two water pressure outlets were constructed at the base of the spiral grooves to apply pore-water pressure into the water compartment and, subsequently, into the soil specimen through the high-air-entry ceramic disk. In addition, a protruding air pressure outlet was placed on top of the grooves to apply pore-air pressure, which is passed through the ceramic disk and into the soil specimen through the porous metal. Therefore, the top cap and pedestal each have three pressure outlets. There are six different valves which connect the pressure outlets to the triaxial cell base. There is another valve at the triaxial cell base which is connected to the cell pressure control. Therefore, the triaxial cell base has seven valves.

Two types of high-air-entry ceramic disk with air-entry value of 1 bar and 5 bar with a thickness of 7.14 mm were used in this study. The 1-bar ceramic disk was used to measure the unsaturated permeability of the soil mixtures up to a suction of 100 kPa, and the 5-bar ceramic disk was used to measure the unsaturated permeability of the soil mixtures up to a suction of 500 kPa. The selection of ceramic disk was based on the saturated permeability of the disks and the applied matric suction to the soil specimens.

The high-air-entry ceramic disk was saturated (Rahimi 2015) before starting the test. The soil specimen prepared with a height of 30 mm and a diameter of 50 mm was set in the triaxial permeameter and it was saturated by applying incremental back pressure and cell pressure. In order to
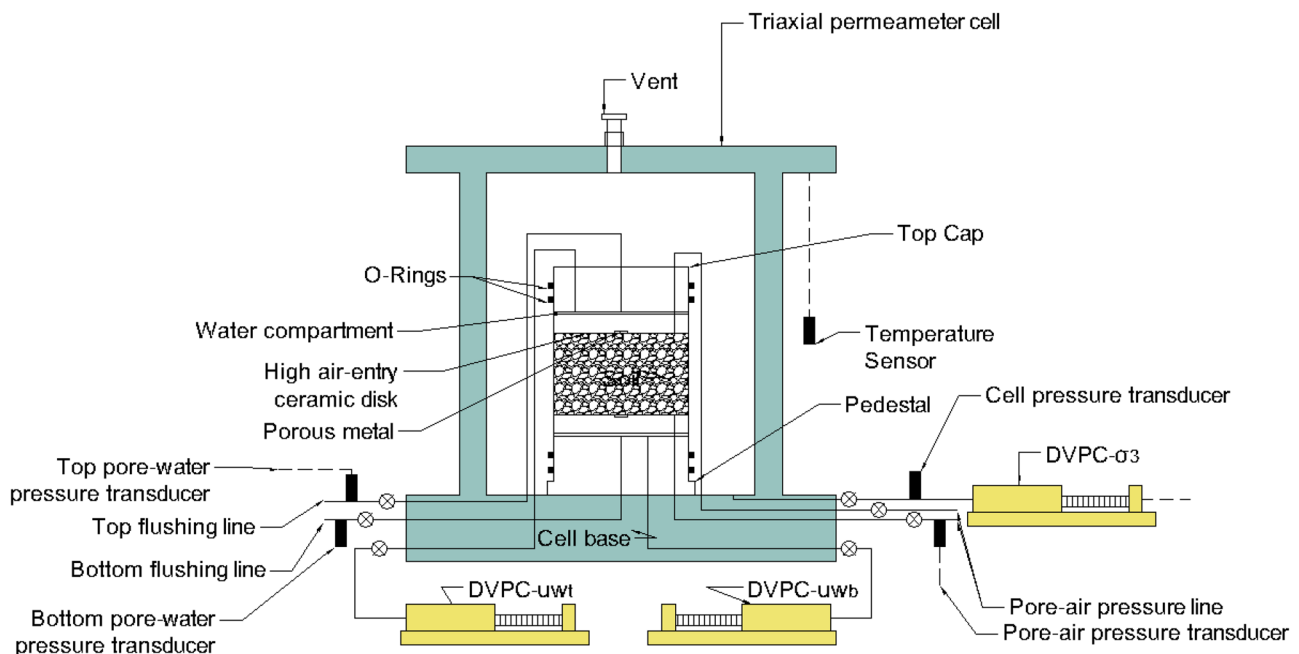

Fig. 1 Schematic diagram of triaxial permeameter used in this study

simulate zero net confining pressure throughout the test, the net confining pressure (σ_3-u_a) was kept small enough (i.e., 10 kPa). The unsaturated permeability test was continued by applying matric suction to the soil specimen. The air pressure lines were connected to the air pressure supply and the pore-water pressure lines were connected to the DPVCs. The air pressure was kept constant during the test, while the pore-water pressure was decreased to the designated value. The cell pressure was also kept constant in order to maintain a constant net confining pressure. The water volume change and total volume change were measured by their respective DPVCs. When changes in water volume ceased, the equilibrium condition was achieved. The subsequent increase in the matric suction was achieved by decreasing the pore-water pressure to the desired values. Once the equilibrium condition was achieved under the designated matric suction, the unsaturated permeability was measured by creating a hydraulic gradient. In order to create the designated hydraulic gradient, two DPVCs were used to apply and control the pore-water pressures at the top and bottom of the soil specimen. The hydraulic gradient was created by decreasing the pore-water pressure at the top of the soil specimen via the connected DPVC which resulted in an upward flow of water through the soil specimen. It should be noted that decreasing the pore-water pressure at the top of the soil specimen will result in non-uniform matric suction distribution through the soil specimen. However, the error is little or negligible when the imposed difference in suction between the top and bottom boundaries is small compared to the mean value of suction. In addition, in a study conducted by Samingan et al. (2003), it was mentioned that unsaturated permeability is not sensitive to the magnitude of hydraulic gradient especially at high matric suction values. Although an excessively high hydraulic gradient is not advisable, the use of a low hydraulic gradient when measuring very low coefficients of permeability is not desirable since the testing time will increase significantly. The inflow and outflow water volume rates from the top and bottom of the soil specimen were continuously measured by the two DPVCs. A graph of the volume rate of flow, q (m^3/s) against time was plotted from the beginning of the test for the top water outflow and the bottom water inflow (see Fig. 2).

A steady-state condition was achieved when the inflow and outflow rates were approximately the same. The test was continued till water flowed at a constant rate for a given period of time.

The bottom high-air-entry disk, soil specimen, and top high-air-entry disk were considered as a three-layered system to take into account the impedance of the ceramic disks (Samingan 2001) and the unsaturated permeability of the soil, k_w, can be computed according to Eq. (1):
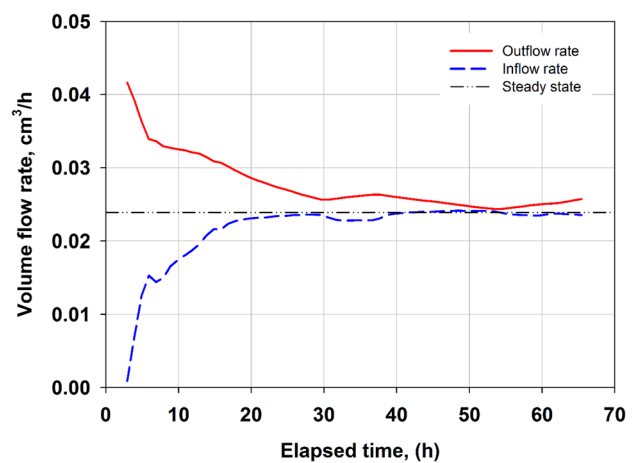

Fig. 2 Steady-state flow condition of soil mixture 100K0S at an applied matric suction of 200 kPa and a hydraulic gradient of 27 in triaxial permeameter

$$k_w = \frac{L_s}{\left(\frac{L}{k} - \left(\frac{L_t}{k_t} + \frac{L_b}{k_b}\right)\right)} \tag{1}$$

where L is the total length of the three layers and k is the total unsaturated permeability, L_s is the length of the soil specimen, L_t is the length of the top disk, L_b is the length of the bottom disk, k_w is the permeability of the soil, k_t is the permeability of the top disk, and k_b is the permeability of the bottom disk.

Results and discussions

Measured SWCC and unsaturated permeability of all the soil mixtures

The results of the SWCC tests of all the soil mixtures are shown in Fig. 3.

The volume change of the soil mixtures 100K0S, 90K10S, 80K20S, and 50K50S was taken into account by using the shrinkage test results (Rahimi 2015).

Figure 4 shows the results of the direct measurement of the unsaturated permeability of all soil mixtures. The unsaturated permeability data, k_w, are plotted versus suction on a semi-log plot.

As shown in the figure, the unsaturated permeability decreased significantly as the suction applied to the soil increased. The permeability of 100K0S, 90K10S, 80K20S, 50K50S, and 20K80S soil mixtures varied from 1.78×10^{-8} (m/s) to 1.89×10^{-11} (m/s), 8.02×10^{-8} (m/s) to 7.05×10^{-11} (m/s), 1.67×10^{-7} (m/s) to 1.60×10^{-11} (m/s), 2.7×10^{-7} (m/s) to 6.19×10^{-12} (m/s), and 8.8×10^{-7} (m/s) to 9.68×10^{-12} (m/s) for the condition from fully saturation
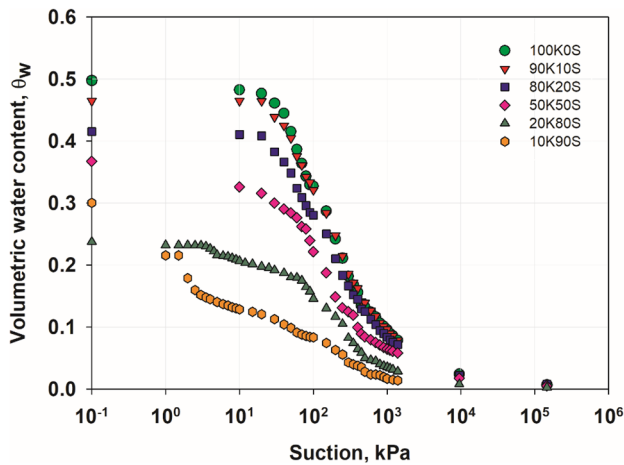
Fig. 3 SWCC of six kaolin-sand soil mixtures in terms of volumetric water content versus suction

to a suction value of 400 kPa, respectively. The permeability of 10K90S soil mixture varied from 1.27×10^{-5} (m/s) to 2.16×10^{-12} (m/s) from fully saturation to a suction value of 300 kPa. It is evident from the results that the reduction in the unsaturated permeability compared to the saturated permeability significantly increases as the sand percentage of the soil mixture increases. The reduction in the unsaturated permeability at a suction of
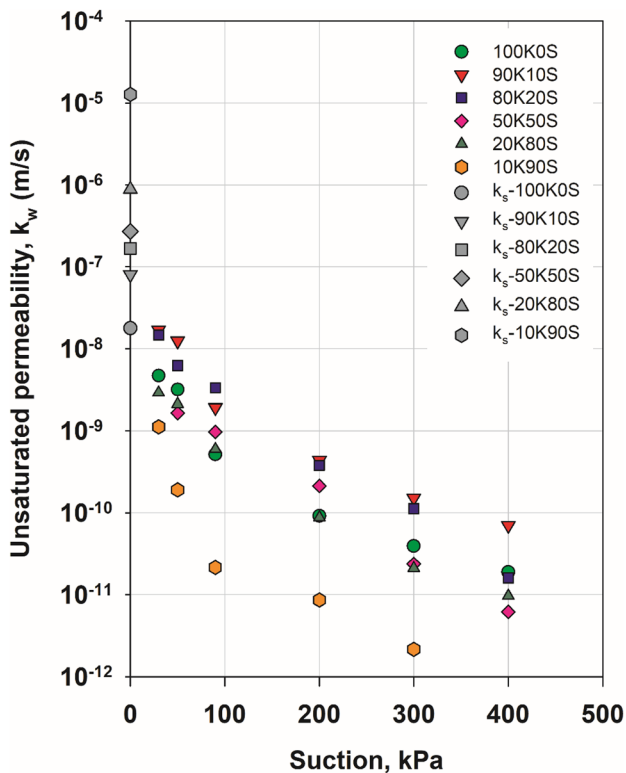
Fig. 4 Measured unsaturated permeability of all the six kaolin-sand soil mixtures

400 kPa compared to the saturated permeability was 2.97, 3.06, 4.02, 4.64, and 4.96 orders of magnitude for 100K0S, 90K10S, 80K20S, 50K50S, and 20K80S soil mixtures, respectively. The reduction at a suction of 300 kPa was 6.77 orders of magnitude for 10K90S soil mixture. It can be seen from the results that the triaxial permeameter with the 1-bar ceramic disk was able to measure unsaturated permeability in the range of 1.75×10^{-8} to 7.20×10^{-11} (m/s) and the triaxial permeameter with the 5-bar ceramic disk was able to measure unsaturated permeability in the range of 4.39×10^{-10} to 2.16×10^{-12} (m/s).

It should be noted that the maximum unsaturated permeability that can be obtained using the triaxial permeameter is limited by the saturated permeability of the high-air-entry ceramic disk. ASTM D5084 specified that the saturated permeability of the high-air-entry ceramic disk must be at least two orders higher than the permeability of the soil specimen being measured so the analysis can be performed without considering the impedance of the high-air-entry ceramic disk. However, the impedance of the ceramic disks was taken into account as described by Eq. (1). Therefore, the maximum unsaturated permeability that can be obtained from the triaxial permeameter with 1-bar and 5-bar ceramic disk in this study was limited to 1.86×10^{-8} (m/s) and 4.68×10^{-10} (m/s), respectively. On the other hand, the minimum unsaturated permeability that can be obtained using the triaxial permeameter is limited by the air-entry value of the ceramic disk. The maximum suction value that can be applied in the triaxial permeameter with 1-bar and 5-bar ceramic disk in this study is limited to 100 kPa and 500 kPa, respectively. If the applied suction is higher than this limit value, the air will enter the ceramic disk and the water compartments in the top cap and pedestal, resulting in unreliable measurements. This limit value corresponds to the maximum suction that can be applied to the soil specimen or the minimum unsaturated permeability of the soil that can be measured. Therefore, measurement of unsaturated permeability near saturation (i.e., near the air-entry value of the soil) for the 50K50S, 20K80S, and 10K90S soil mixtures was not reliable since their saturated permeabilities (i.e., 2.7×10^{-7} (m/s), 8.8×10^{-7} (m/s), and 1.27×10^{-5} (m/s), respectively) were higher than the saturated permeability of the 1-bar ceramic disk (i.e., 1.86×10^{-8} (m/s)).

Comparison between directly measured and estimated unsaturated permeability data of the soil mixtures

The unsaturated permeability of the soil mixtures was estimated using the matrix of unsaturated permeability estimation model developed by Rahimi et al. (2015a). First, the complete measured SWCC data of the soil mixtures were used as the input for the estimation. Second, the measured SWCC data up to 100 kPa suction were used as the input for the estimation. Third, the measured SWCC data up to

Table 3 Computed RMSE values for soil mixtures of this study for the complete measured SWCC data, the measured SWCC data up to 100 kPa, and the measured SWCC data up to 100 kPa suction in combination with the estimated SWCC data points

|	Soil mixture	Model									
		F&X-1994	VG-1980	FCM	FMM	FCM C(ψ) = 1	FMM C(ψ) = 1	VCM m = 1−1/n	VMM m = 1−1/n	VCM	VMM
Complete measured SWCC	100K0S	0.388	1.091	0.392	1.035	0.426	1.185	0.333	0.691	0.384	0.542
	90K10S	0.650	0.531	0.641	0.433	0.575	0.508	0.747	0.310	0.850	0.423
	80K20S	1.151	0.600	1.075	0.447	1.087	0.450	1.501	0.870	1.497	0.864
	50K50S	1.637	1.208	1.475	0.692	1.390	0.623	2.216	1.585	1.384	0.622
	20K80S	1.901	2.243	1.178	0.626	1.195	0.627	3.395	2.672	1.183	0.604
	10K90S	2.624	1.257	1.303	0.908	1.312	0.901	1.023	0.628	1.239	0.832
	Average	1.392	1.155	1.011	0.690	0.997	0.715	1.536	1.126	1.089	0.648
	Standard deviation	0.831	0.616	0.413	0.243	0.401	0.277	1.118	0.868	0.409	0.170
Measured SWCC data up to 100 kPa	100K0S	0.987	3.115	1.126	1.973	0.852	1.069	1.923	2.252	14.199	14.707
	90K10S	0.636	4.985	0.629	0.649	0.964	0.997	3.450	3.693	2.481	2.684
	80K20S	1.063	2.448	1.000	0.673	1.048	0.840	1.441	1.614	8.073	8.559
	50K50S	1.124	1.520	0.693	0.861	0.646	0.954	0.683	0.788	0.681	0.929
	20K80S	0.613	3.396	0.818	1.332	0.868	1.450	0.831	1.393	0.750	1.172
	10K90S	2.765	3.571	1.443	1.038	0.745	0.918	1.524	1.952	0.429	0.432
	Average	1.198	3.172	0.952	1.088	0.854	1.038	1.642	1.949	4.435	4.747
	Standard deviation	0.798	1.162	0.304	0.502	0.145	0.216	0.998	0.990	5.588	5.726
Measured SWCC data up to 100 kPa and estimated points	100K0S	0.670	1.056	0.663	1.140	0.666	0.881	0.676	0.637	0.614	0.692
	90K10S	0.698	0.530	0.696	0.454	0.663	0.462	0.736	0.301	0.871	0.534
	80K20S	1.142	0.598	1.066	0.441	1.144	0.449	1.489	0.864	1.525	0.933
	50K50S	1.208	1.277	0.737	0.694	0.756	0.669	2.281	1.654	0.716	0.742
	20K80S	2.106	1.840	1.392	0.696	1.382	0.694	3.047	2.304	1.357	0.693
	10K90S	1.009	2.217	0.766	0.602	0.804	1.019	0.605	0.416	1.024	1.019
	Average	1.139	1.253	0.887	0.671	0.903	0.696	1.472	1.029	1.018	0.769
	Standard deviation	0.523	0.673	0.287	0.255	0.294	0.226	1.006	0.788	0.360	0.177
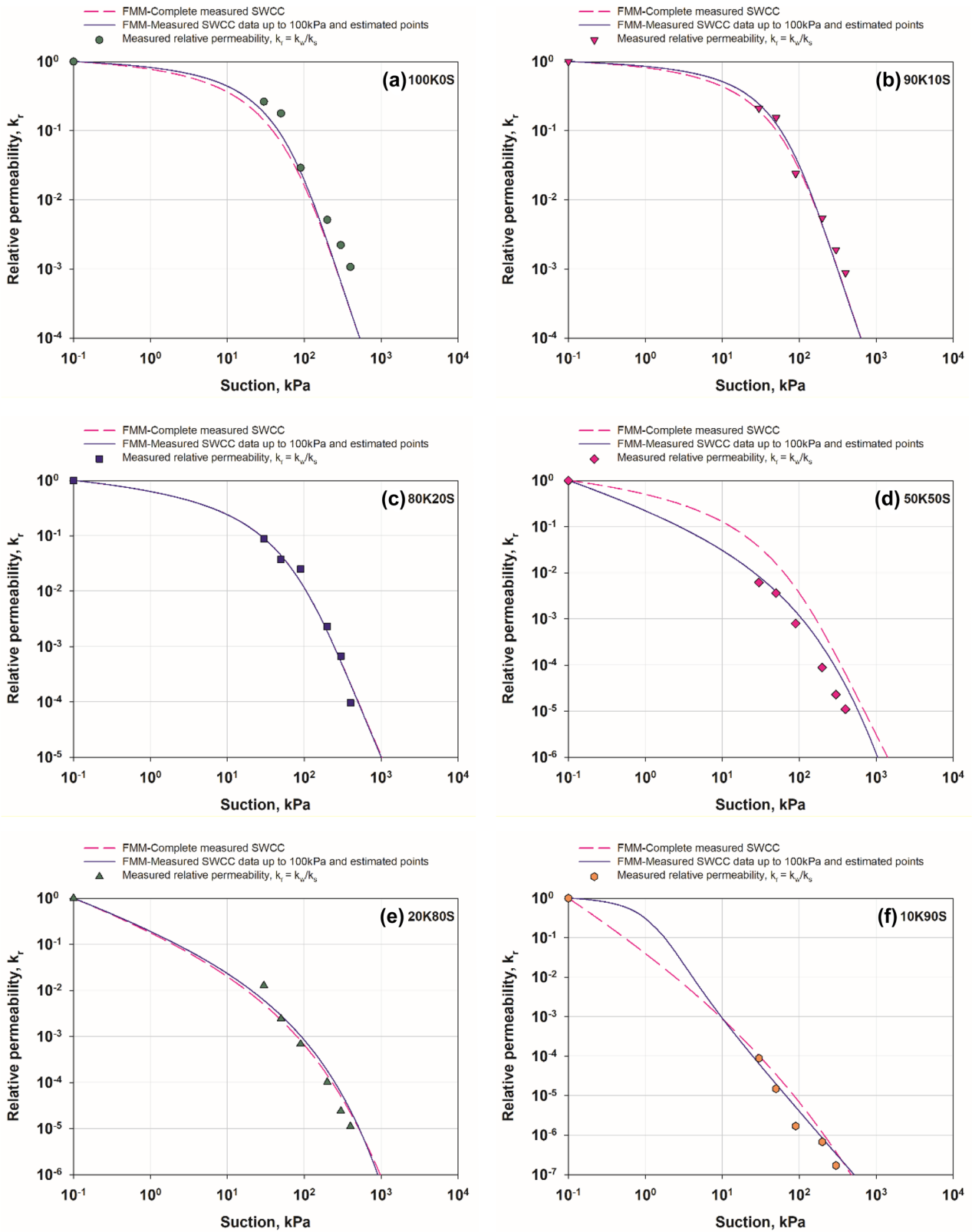
Fig. 5 Directly measured unsaturated permeability data versus estimated unsaturated permeability by FMM using the complete measurements of SWCC data and using the measured SWCC data up to 100 kPa suction in combination with the estimated SWCC data points beyond 100 kPa

100 kPa suction in combination with the estimated SWCC data points were used as the input for the estimation. The deviation between the directly measured unsaturated permeability of the soil mixtures in this study and their respective estimated unsaturated permeability was calculated using the root mean square error (RMSE) following Eq. (2).

$$RMSE = \sqrt{\sum_{i=1}^{i=X} \left(\log(k_{ri}) - \log(\widehat{k}_{ri}) \right)^2} \tag{2}$$

where k_r is the measured unsaturated permeability value, $\widehat{k}_r$ is the estimated unsaturated permeability value, X is the number of measured data points, and i is a counter. A lower RMSE value shows a better fit to the measured data.

Table 3 shows the computed RMSEs for the estimated unsaturated permeabilities using the complete measurement of SWCC data, the measured SWCC data up to 100 kPa suction, and the measured SWCC data up to 100 kPa suction in combination with the estimated SWCC data points. The average and standard deviation of RMSE values of all the soil mixtures are also shown in the table.

The average (standard deviation) of the RMSEs of all the soils and all the models was 1.036 (SD = 0.63) and 2.107 (SD = 2.79) for the complete measurement of SWCC data and the SWCC data up to 100 kPa suction, respectively. It means that, when the best-fit SWCCs using the complete measurement of SWCC data was used for estimation, the unsaturated permeability estimation models had a better fit to the directly measured unsaturated permeability data, as shown by the lower values of RMSEs.

The average and standard deviation of the RMSEs of all the soils and all the models was 0.983 (SD = 0.54) for the measured SWCC data up to 100 kPa suction in combination with the estimated SWCC data points beyond 100 kPa which was similar to that of the complete measurements of SWCC data (i.e., 1.036 (SD = 0.63)). Therefore, it can be concluded that the third method which used the measured SWCC data up to 100 kPa suction in combination with the estimated SWCC data points beyond 100 kPa suction as proposed by Rahimi and Rahardjo (2015) provided a good fit to the directly measured unsaturated permeability data of this study.

To illustrate the results, the directly measured unsaturated permeability data versus the estimated unsaturated permeability data using the complete measurements of SWCC data and the measured SWCC data up to 100 kPa suction in combination with the estimated SWCC data points beyond 100 kPa for FMM estimation model for all the soil mixtures used in this study are shown in Fig. 5.

The coefficient of determination R^2 was computed according to Eq. (3) for all data points measured directly.

$$R^2 = 1 - \frac{SSE}{SST} \tag{3}$$

where $SST = \sum_{i=1}^{X} \left(k_{wi} - \bar{k}_w \right)^2$, $SSE = \sum_{i=1}^{X} \left(k_{wi} - \widehat{k}_{wi} \right)^2$, and $\bar{k}_w$ is the average measured unsaturated permeability, $\widehat{k}_{wi}$ is the estimated unsaturated permeability, k_{wi} is the measured unsaturated permeability, X is the number of data points, and i is a counter.
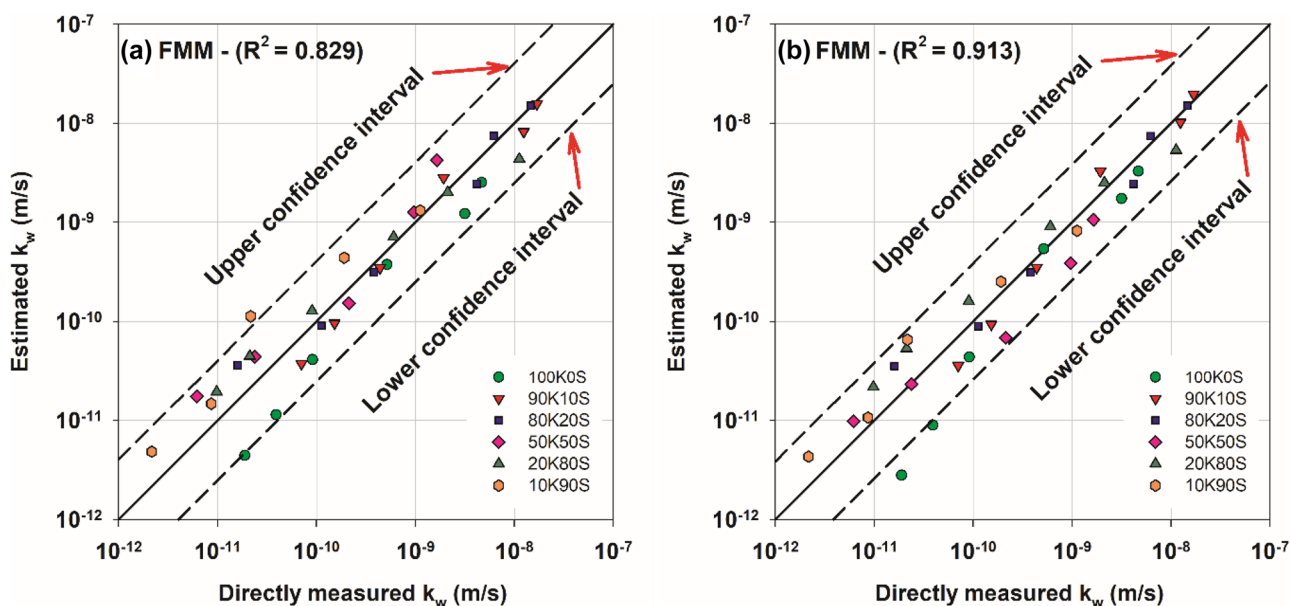

Fig. 6 Directly measured unsaturated permeability data versus estimated unsaturated permeability by FMM (**a**) using the complete measurements of SWCC data (**b**) using the measured SWCC data up to 100 kPa suction in combination with the estimated SWCC data points beyond 100 kPa

The values of R^2 as shown in Fig. 6a, b were 0.829 and 0.913 for the complete measurements of SWCC data and the measured SWCC data up to 100 kPa in combination with estimated SWCC data points, respectively. The high values of R^2 show the ability of FMM model to reasonably fit the directly measured data.

Equation (4) was used to compute the 95% confidence interval of the observed errors, $\left(k_{wi} - \widehat{k}_{wi}\right)$, between the two sets of data (i.e., measured versus estimated), and is shown in Fig. 6a, b by two dashed lines.

$$\mu\left(k_{wi} - \widehat{k}_{wi}\right) \pm Z_{\alpha/2}\sigma\left(k_{wi} - \widehat{k}_{wi}\right) \tag{4}$$

where $\mu = \frac{1}{X}\sum_1^X k_{wi}$, $\sigma = \sqrt{\frac{1}{X}\sum_1^X (k_{wi} - \mu)^2}$ and α is the significance level.

The 95% confidence interval of the observed error were $(-0.614, 0.597)$ and $(-0.535, 0.635)$, creating a range of 1.21 and 1.17 in orders of magnitude, for the complete measurements of SWCC data and the measured SWCC data up to 100 kPa in combination with estimated SWCC data points, respectively. It means both approach could reasonably fit the directly measured unsaturated permeability data.

Conclusions

Based on the experimental results of the directly measured unsaturated permeability data of six different kaolin-sand mixtures and their estimated unsaturated permeability data, it can be concluded that the unsaturated permeability estimation models could reasonably fit the directly measured unsaturated permeability data when both the complete measured SWCC data and the measured SWCC data up to 100 kPa suction in combination with the estimated SWCC data at higher suction values were used.

Declarations

References

ASTM (1997) D2487: Standard Classification of Soils for Engineering Purposes (Unified Soil Classification System). ASTM International, West Conshohocken, PA, USA

ASTM (2003) D5084: standard test methods for measurement of hydraulic conductivity of saturated porous materials using a flexible wall permeameter. ASTM International, West Conshohocken, PA, USA

Bhaskar P, Puppala AJ, Boluk B (2022) Influence of unsaturated hydraulic properties on transient seepage and stability analysis of an earthen dam. Int J Geomech 22(7). https://doi.org/10.1061/(ASCE)GM.1943-5622.0002414

Brutsaert W (1966) Probability laws for pore-size distributions. Soil Sci 101(2):85–92

Chaminda G, Jayantha K, Taro U (2013) Laboratory measurement of hydraulic conductivity functions of two unsaturated sandy soils during drying and wetting processes. Soils Found 53(3):417–430. https://doi.org/10.1016/j.sandf.2013.04.004

Cihan A, Tyner JS, Perfect E (2009) Predicting relative permeability from water retention: a direct approach based on fractal geometry. Water Resour Res 45(4). https://doi.org/10.1029/2008WR007038

Fredlund DG, Rahardjo H (1993) Soil mechanics for unsaturated soils. Wiley, New York

Fredlund DG, Xing A (1994) Equations for the soil-water characteristic curve. Can Geotech J 31:521–532. https://doi.org/10.1139/t94-061

Fredlund DG, Xing A, Huang S (1994) Predicting the permeability function for unsaturated soils using the soil-water characteristic curve. Can Geotech J 31(4):533–546. https://doi.org/10.1139/t94-062

Goh SG, Rahardjo H, Leong EC (2015) Modification of triaxial apparatus for permeability measurement of unsaturated soils. Soils Found 55(1):63–73. https://doi.org/10.1016/j.sandf.2014.12.005

Hilf Jack W (1956) An investigation of pore-water pressure in compacted cohesive soils. University of Colorado, PhD

Liang C, Cao C, Wu S (2018) Hydraulic-mechanical properties of loess and its behavior when subjected to infiltration-induced wetting. Bull Eng Geol Environ 77:385–397. https://doi.org/10.1007/s10064-016-0943-x

Mualem Y (1976) New model for predicting the hydraulic conductivity of unsaturated porous media. Water Resour Res 12(3):513–522. https://doi.org/10.1029/WR012i003p00513

Pandey P, Lynch K, Sivakumar V, Solan B, Tripathy S, Nanda S, Donohue S (2021) Measurements of permeability of saturated and unsaturated soils. Géotechnique 71(2):170–177. https://doi.org/10.1680/jgeot.19.P.058

Rahimi A (2015) Parameters affecting estimation of unsaturated permeability of soils. PhD. Nanyang Technological University, Singapore

Rahimi A, Rahardjo H (2015) A new approach to improve soil-water characteristic curve to reduce variation in estimation of unsaturated permeability function. Can Geotech J 53(4):717–725. https://doi.org/10.1139/cgj-2015-0199

Rahimi A, Rahardjo H, Leong EC (2015a) Effect of soil-water characteristic curve and relative permeability equations on estimation of unsaturated permeability of soils. Soils and Founds 55(6):1400–1411. https://doi.org/10.1016/j.sandf.2015.10.006

Rahimi A, Rahardjo H, Leong EC (2015b) Effect of range of soil–water characteristic curve measurements on estimation of permeability function. Eng Geol 185:96–104. https://doi.org/10.1016/j.enggeo.2014.11.017

Samingan AS (2001) Hydraulic properties of residual soils. MEng. Nanyang Technological University, Singapore

Samingan AS, Leong EC, Rahardjo H (2003) A flexible wall permeameter for measurements of water and air coefficients of permeability of residual soils. Can Geotech J 40(3):559–574. https://doi.org/10.1139/t03-015

Samingan AS, Leong EC, Rahardjo H (2005) Estimating permeability functions of Singapore residual soils. Eng Geol 78(1–2):119–133. https://doi.org/10.1016/j.enggeo.2004.12.001

van Genuchten MT (1980) Closed-form equation for predicting the hydraulic conductivity of unsaturated soils. Soil Sci Soc Am J 44(5):892–898. https://doi.org/10.2136/sssaj1980.03615995004400050002x